Type Ia supernovae and their explosive nucleosynthesis: Constraints on progenitors

Shing-Chi Leung

Department of Mathematics and Physics, SUNY Polytechnic Institute, 100 Seymour Road, Utica, New York 13502, USA
TAPIR, Mailcode 350-17, California Institute of Technology, Pasadena, CA 91125, USA
E-mail: leungs@sunypoly.edu
https://sunypoly.edu/faculty-and-staff/shing-chi-leung.html

Ken'ichi Nomoto

Kavli Institute for the Physics and Mathematics of the Universe (WPI), The University of Tokyo Institutes for Advanced Study, The University of Tokyo, Kashiwa, Chiba 277-8583, Japan
E-mail: nomoto@astron.s.u-tokyo.ac.jp

What the progenitors of Type Ia supernovae (SNe Ia) are, whether they are near-Chandrasekhar mass or sub-Chandrasekhar mass white dwarfs, has been the matter of debate for decades. Various observational hints are supporting both models as the main progenitors. In this paper, we review the explosion physics and the chemical abundance patterns of SNe Ia from these two classes of progenitors. We will discuss how the observational data of SNe Ia, their remnants, the Milky Way Galaxy, and galactic clusters can help us to determine the essential features where numerical models of SNe Ia need to match.

Keywords: Supernova; Hydrodynamics; Nucleosynthesis; Supernova Remnant; Galactic Chemical Evolution

1. Introduction

Type Ia supernovae (SNe Ia) are well-understood as the thermonuclear explosions of carbon-oxygen white dwarfs (CO WDs).[1–3] They produce the majority of iron-peak elements in the galaxy, in particular ^{55}Mn. Their light curves can be standardized for measuring distance in the cosmological scale.[4,5] Understanding their progenitors, the explosion mechanisms and their obseravables are important for understanding the Universe in the larger scale.[6,7] In this review paper, we will explore possible progenitors of SNe Ia, whether they are the explosions of near-Chandrasekhar mass (Ch-mass) WDs or sub-Chandrasekhar mass (subCh-mass) WDs. In Table 1 we tabulate the important features to contrast between the Ch-mass and subCh-mass WDs.

The rise of the two classes of models comes from the diversity of observed SNe Ia. In the literature, a number of explosion models have been proposed to explain the normal and peculiar SNe Ia. For the Ch-mass WD, representative models include the pure turbulent deflagration model (PTD),[8–15] PTD with deflagration-detonation transition,[16–22] gravitationally confined detonation model[23–27] and pulsation reverse

detonation models.[28,29] The subCh-mass WD models include the double-detonation model,[30–38] violent merger model[39–42] and WD head-on collision model.[43–45] On top of these, unconventional models such as magnetized WDs,[46] super-Chandrasekhar mass WDs,[47] differentially rotating WDs[48,49] and interaction with dark matter gravity[50,51] have been proposed to explain some unusual SNe Ia.

Table 1. Comparing essential features of Ch-mass and subCh-mass WDs.

	unit	Ch-mass WD	subCh-mass WD
mass	$M_\odot$	$1.30 - \geqslant 1.38$	0.9 – 1.2
central density	g cm^{-3}	$10^9 - 10^{10}$	10^7 – 10^8
composition		^{12}C+^{16}O+^{22}Ne	core: ^{12}C+^{16}O+^{22}Ne envelope (env): ^{4}He
reaction		subsonic deflagration	supersonic detonation
first site		(near-)center	off-center (He-env)

The study of SNe Ia as explosions of (sub)Ch-mass WDs is often linked to the open question about the progenitors of SNe Ia: the single degenerate (SD) vs. the double degenerate (DD) scenario. The SD scenario means that the primary WD develops its nuclear runaway by mass accretion from its companion star, which can be a slightly evolved main-sequence, a red-giant, or a He-star.[49,52] The DD scenario means that the primary WD triggers the runaway by dynamical interaction with its companion WD.

We remind that the question on whether SNe Ia develop from Ch-mass WDs is not equivalent to arguing SNe Ia mainly develop in the SD scenario. For example, in the SD scenario, when the WD explodes as an SN Ia depends on the mass accretion rate from its companion star and the WD initial mass (see the left panel of Figure 1). A WD having (1) a high mass accretion rate above $\sim 10^{-9}$ $M_\odot$ yr^{-1} or (2) having a low mass accretion rate and a high initial mass > 1.1 $M_\odot$ is likely to develop nuclear runaway in the Ch-mass limit. Otherwise, the WD is more likely to explode as a subCh-mass WD.[53] Similar features have been seen also for WDs in the DD scenario.

To understand why the C-deflagration is associated with the Chandrasekhar mass WD, we show in the right panel of Figure 1 the relative pressure change of the CO-rich matter as a function of the matter density. During the thermonuclear runaway, ^{12}C and ^{16}O burn to form iron-peak elements peaked at ^{56}Ni, releasing an amount of $\sim 10^{18}$ erg g^{-1}. When the density is high ($\sim 10^9$ g cm^{-3}), the electron degeneracy pressure dominates the matter pressure, and the overall pressure becomes insensitive to its temperature. As a result, the relative pressure jump decreases as the matter becomes more degenerate. Without an abrupt pressure jump, the nuclear runaway in the Ch-mass WD may not spontaneously trigger a shock wave and hence no detonation may form. The hot matter may ignite ^{12}C in the nearby cold matter only by thermal conduction.

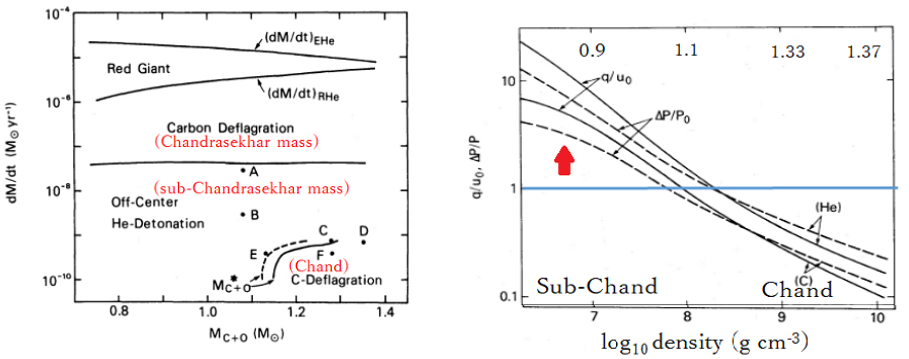

Fig. 1. (left panel) The final fate of the WD in the SD scenario with the mass accretion rate and the initial CO WD mass as parameters (derived and edited from Ref. 53). (right panel) The relative pressure change $\Delta P/P_0$ and relative internal energy change q/u_0 before and after nuclear runaway as a function of the matter density for the He-rich (solid line) and CO-rich (dashed line) matter (Ref. 30). The numbers on the top corresponds to the mass of the WD when the density corresponds to the central density of the WD. The red arrow indicates the relative pressure change of the CO-rich matter.

Unlike the detonation, the subsonic deflagration is subject to hydrodynamical instabilities such as the Rayleigh-Taylor (RT), Kelvin-Helmholtz (KH) and Landau-Derrieus[54–56] instabilities. The analytic model suggests that the buoyancy force can drive the early flame away from the center.[57] In Figure 2 we plot the electron fraction Y_e profile of a canonical PTD model where the deflagration has quenched after the expansion of the WD. The Y_e profile is a useful scalar for tracking how the fluid elements move inside the star. We observe the elongated "mushroom" shape as features of the RT-instabilities and the spiral along and inside the "mushrooms" as features of the KH-instabilities.

However, a WD may not naturally explode if there is only a slow subsonic nuclear flame because the WD expands and quenches the flame before the whole WD is burnt.[8,12] To alleviate this issue, a deflagration-detonation transition[16] and a flame-acceleration scheme[9,58,59] have been proposed for assisting nuclear burning to spread around the entire WD before the WD expands.

2. Typical Type Ia Supernova Explosion

Both the Ch-mass and subCh-mass WD models have their individual strengths and concerns, despite both of them can reproduce the observed features of normal SNe Ia,[60–62] including the Philip's relation.[37,63] For example, the Ch-mass model can produce Mn with an amount consistent with the solar abundance,[64] while the subCh-mass models do not produce a significant amount of Mn. But the DDT mechanism remains a matter of debate whether or not the turbulence is sufficient to pre-condition the CO rich matter.[57,65–69]

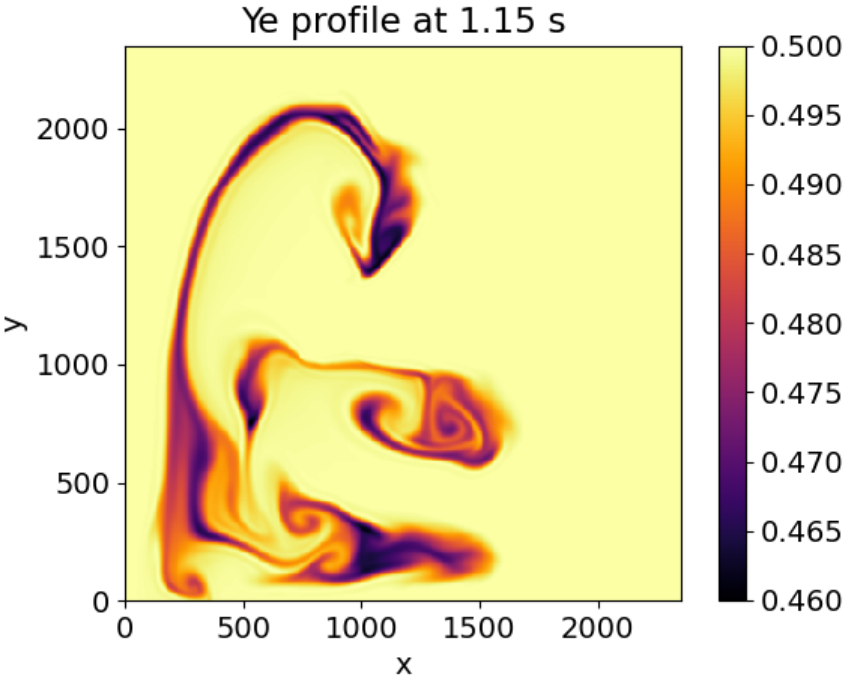

Fig. 2. A snapshot of the electron fraction Y_e profile in a typical PTD model demonstrating simultaneously the Rayleigh-Taylor and Kelvin-Helmholtz instabilities due to interaction of turbulent fluid motion with the deflagration front.

2.1. *Typical Explosion Mechanism of Ch-mass and subCh-mass Models*

We now examine the typical explosion mechanism in both the Ch-mass and subCh-mass WDs. Even though we have described a number of explosion mechanisms in the previous section, in general they are only different by the progenitor or the initial explosion kernel. The underlying mechanism, namely the deflagration and detonation, remains unchanged. Here we examine how the WD explodes accordingly.

In Figures 3 and 4 we plot the temperature profiles of the representative Ch-mass WD explosion using the PTD model with DDT for a WD of 1.37 $M_\odot$, metallicity $Z = 0.02$ and a $c3$ deflagration kernel[22] based on two-dimensional simulations.[70] The WD is burnt by subsonic flame for around 1 s, consuming about $\sim 30\%$ of the CO-rich matter in mass. After that, DDT is assumed to take place and the remaining matter is burnt within ~ 0.1 s. Eventually, the WD undergoes homologous expansion which quenches both deflagration and detonation.

In Figures 5 and 6 we plot similar profiles to Figure 3-4 but for the subCh-mass model with the initial mass 1.10 $M_\odot$, $Z = 0.02$ and a single He-detonation bubble.[35] In the first 1 s, the detonation burns the He-rich matter along the envelope.

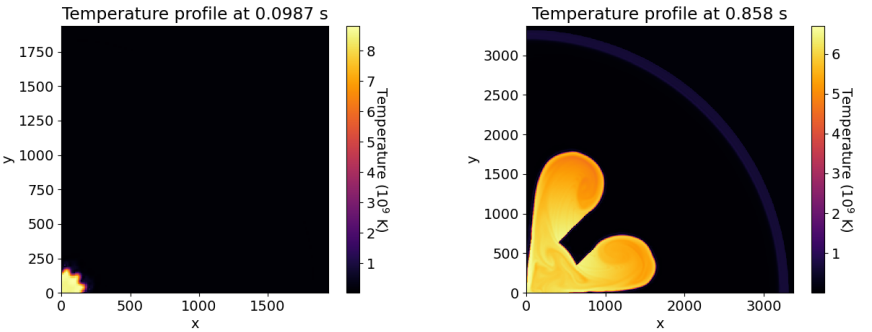

Fig. 3. (left panel) The initial temperature profile of the quadrant cross-section in a typical Ch-mass model using the PTD model with DDT for an initial mass $M = 1.37\ M_{\odot}$, metallicity $Z = 0.02$, and a "three-finger" initial flame kernel.[22] (top right panel) Same as the top left panel when the DDT is assumed to be triggered.

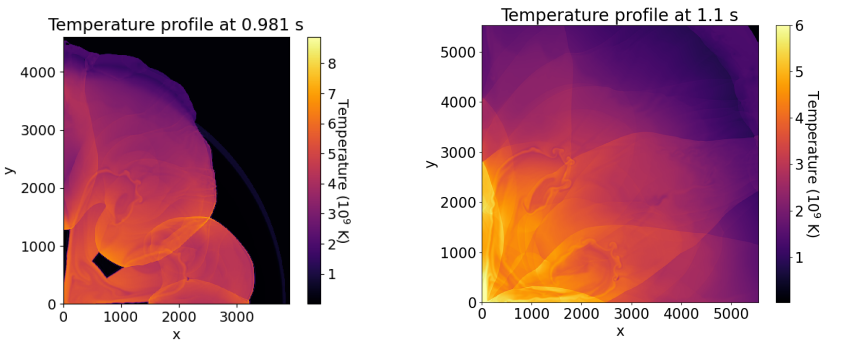

Fig. 4. (left panel) Same as Figure 3 but during the detonation phase. (right panel) Near complete disruption of the WD.

The detonation strength increases during the collision, which creates a shock that penetrates into the CO-core. This creates the C-detonation which later disrupts the entire WD.

2.2. *General Thermodynamical Features*

Typical multi-dimensional SN Ia simulations solve the Eulerian hydrodynamics equations with a simplified nuclear reaction network. To obtain the detailed chemical

Table 2. Major isotopes of iron-peak elements and their corresponding electron fraction.

Isotope	^{54}Fe	^{55}Mn	^{55}Fe	^{55}Fe	^{56}Fe	^{56}Co	^{56}Ni	^{57}Fe	^{58}Ni	^{60}Ni
Ye	0.481	0.454	0.472	0.490	0.464	0.482	0.500	0.456	0.483	0.467

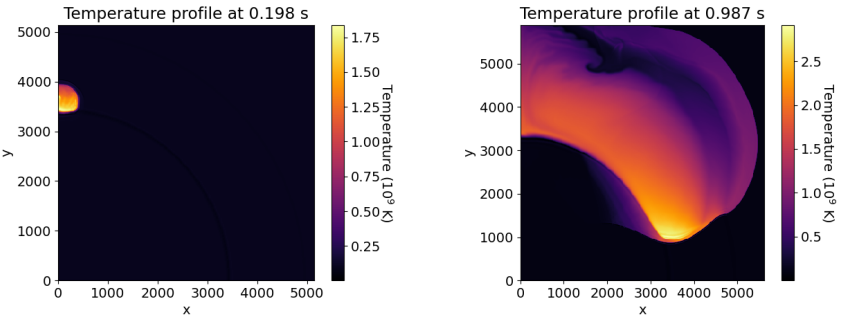

Fig. 5. (left panel) The initial temperature profile of a typical subCh-mass model using the double detonation model with the initial mass $M = 1.10\ M_\odot$, $Z = 0.02$, and a "single bubble" initial detonation kernel.[35] (right panel) Same as the top left panel but during the amplification of the He detonation.

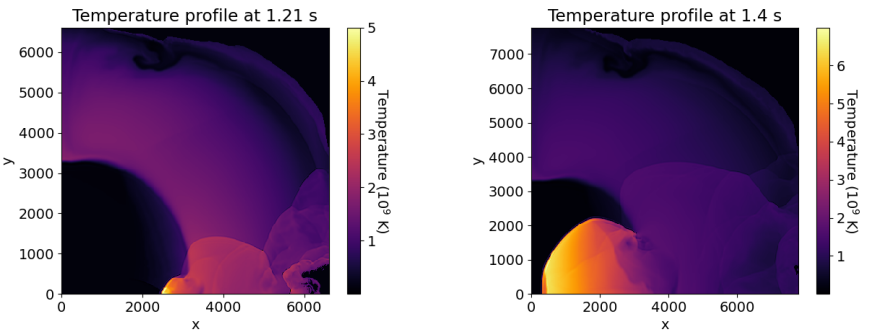

Fig. 6. (left panel) Same as Figure 5 but during the onset of the C-detonation. (right panel) Same as the left panel but during the C-detonation phase.

features of the explosion, a passive tracer particle scheme[71–74] is necessary. This scheme allocates a number of Lagrangian tracers to follow the fluid motion. The notation "passive" means that the tracers do not affect the fluid motion; they only record the thermodynamical condition along their trajectories.

The tracer particles record $(\rho(t), T(t))$ as a Lagrangian fluid packet along its path for reconstructing the exact chemical abundances. For SNe Ia, the trajectory is less convoluted that its peak density and temperature $(\rho_{\rm peak}, T_{\rm peak})$ can characterize the typical nucleosynthesis features inside the tracer. We make numerical experiments to show how various nucleosynthesis quantities depend on the parameters $(\rho_{\rm peak}, T_{\rm peak})$ parameter space.

We assume that the tracers start from given $(\rho_{\rm peak}, T_{\rm peak})$ and then adiabatically expand. The expansion timescale is chosen according to the typical explosion energy 10^{51} erg. The nuclear reactions are computed using the 495-isotope network.[75]

In Figures 7 and 8 we plot the final mean atomic number $\bar{A}$, $Y_{\rm e}$, asymptotic mass fraction of ^{55}Mn and ^{56}Fe for tracers under different initial conditions. The region is

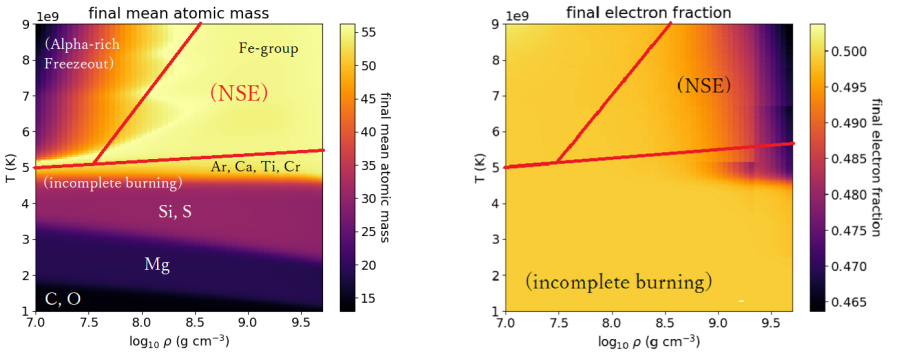

Fig. 7. (left panel) The final mean atomic mass number $\bar{A}$ of the tracer particles starting from different $\rho_{\rm peak}$ and $T_{\rm peak}$ (in units of 10^9 K). (right panel) Same as the left panel, but for the final electron fraction $Y_{\rm e}$ of the tracer.

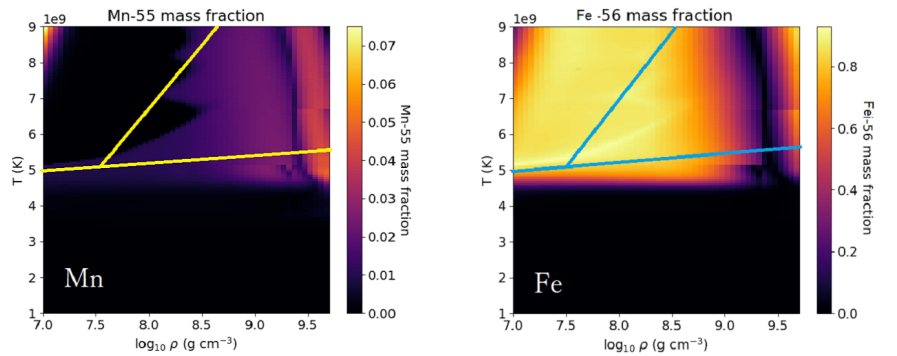

Fig. 8. (left panel) Same as Figure 7, but for the final mass fraction of stable ^{55}Mn. (right panel) Same as the left panel but for the final mass fraction of stable ^{56}Fe.

divided into three regions.[76,77] The low-$\rho_{\rm peak}$ region corresponds to the incomplete Si-burning regime, where the nuclear reaction terminates before reaching Fe-group elements, such as Si, S, Ar and so on. The high-$T_{\rm peak}$ (in units of 10^9 K) and low-$\rho_{\rm peak}$ region corresponds to the α-rich freezeout regime. As the name suggests, the nuclear reaction is confined to be along the α-chain from ^{12}C to ^{56}Ni. The high-$T_{\rm peak}$ and high-$\rho_{\rm peak}$ region corresponds to the nuclear statistical equilibrium (NSE) regime. This regime plays an important role in the Ch-mass WD as it allows isotopes away from the α-chain to form through weak interaction (electron capture).

As the $Y_{\rm e}$-profile indicates, the NSE zone is also the region where matter with $Y_{\rm e} < 0.5$ can be formed. The low $Y_{\rm e}$ environment is vital for forming the parents of ^{55}Mn (see Table 2 for the representative $Y_{\rm e}$ for the major neutron-rich isotopes of iron-peak elements). The ^{55}Mn profile also shows that the NSE zone is the primary site for generating a significant amount of stable ^{55}Mn after decay. On the other hand, ^{56}Fe is mostly formed in the α-rich freezeout and NSE ($Y_{\rm e} \approx 0.5$) regions.

2.3. *Thermodynamical Trajectories of SN Ia Models*

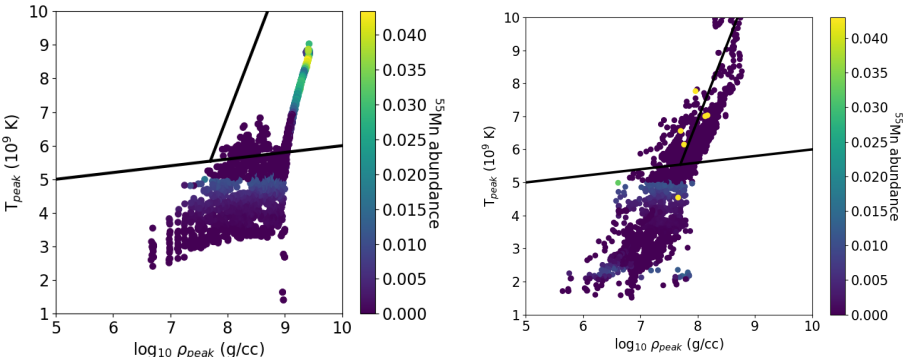

Fig. 9. (left panel) The thermodynamical trajectories of tracer particles of the Ch-mass model with the colour being the asymptotic ^{55}Mn abundance. Same as the left panel but for the subCh-mass model.

Having explored which thermodynamical parameter space is responsible for iron-peak elements, we show in Figure 9 the thermodynamics trajectories of tracers obtained from the typical Ch-mass and subCh-mass models. The chemical abundance of each tracer is directly computed according to its individual (ρ, T) time evolution.

The Ch-mass model (left panel) has two distinctive parts: the high density thin tail and the thick body at low density. At high density ($\rho_{\rm peak} > 10^9$ g cm^{-3}), the tracers are in the NSE regime and have a significantly higher ^{55}Mn and low fluctuations in $T_{\rm peak}$ for the same $\rho_{\rm peak}$. These are the tracers burnt by the subsonic deflagration. The absence of shock ensures that nuclear burning does not generate strong acoustic waves. On the other hand, the majority of tracers burnt by the detonation undergo incomplete Si-burning. The aspherical explosion allows tracers with the same initial mass coordinate to be burnt at a range of time. This leads to a wide temperature range for the same $\rho_{\rm peak}$. There is also a narrow band of tracers for $7 < \log_{10}\rho_{\rm peak} < 9$ and $T_{\rm peak} \approx 5 \times 10^9$ K also responsible for synthesizing a small fraction of ^{55}Mn.

The subCh-mass model (right panel) has a uniform structure where the $T_{\rm peak}$ scales with $\rho_{\rm peak}$ with some fluctuations. Only a small part of tracers reaches the NSE regime but their density is not high enough for the ^{55}Mn synthesis. There is also a narrow band of tracers containing ^{55}Mn by the synthesis of ^{55}Co. In general the global ^{55}Mn in the subCh-mass model is lower than that of the Ch-mass model.

2.4. *Typical Nucleosynthesis in Ch-mass and subCh-mass Models*

Now we have examined the thermodynamical differences between the Ch-mass and subCh-mass WDs. In Figure 10 we compare the qualitative differences in the nucleosynthesis pattern.

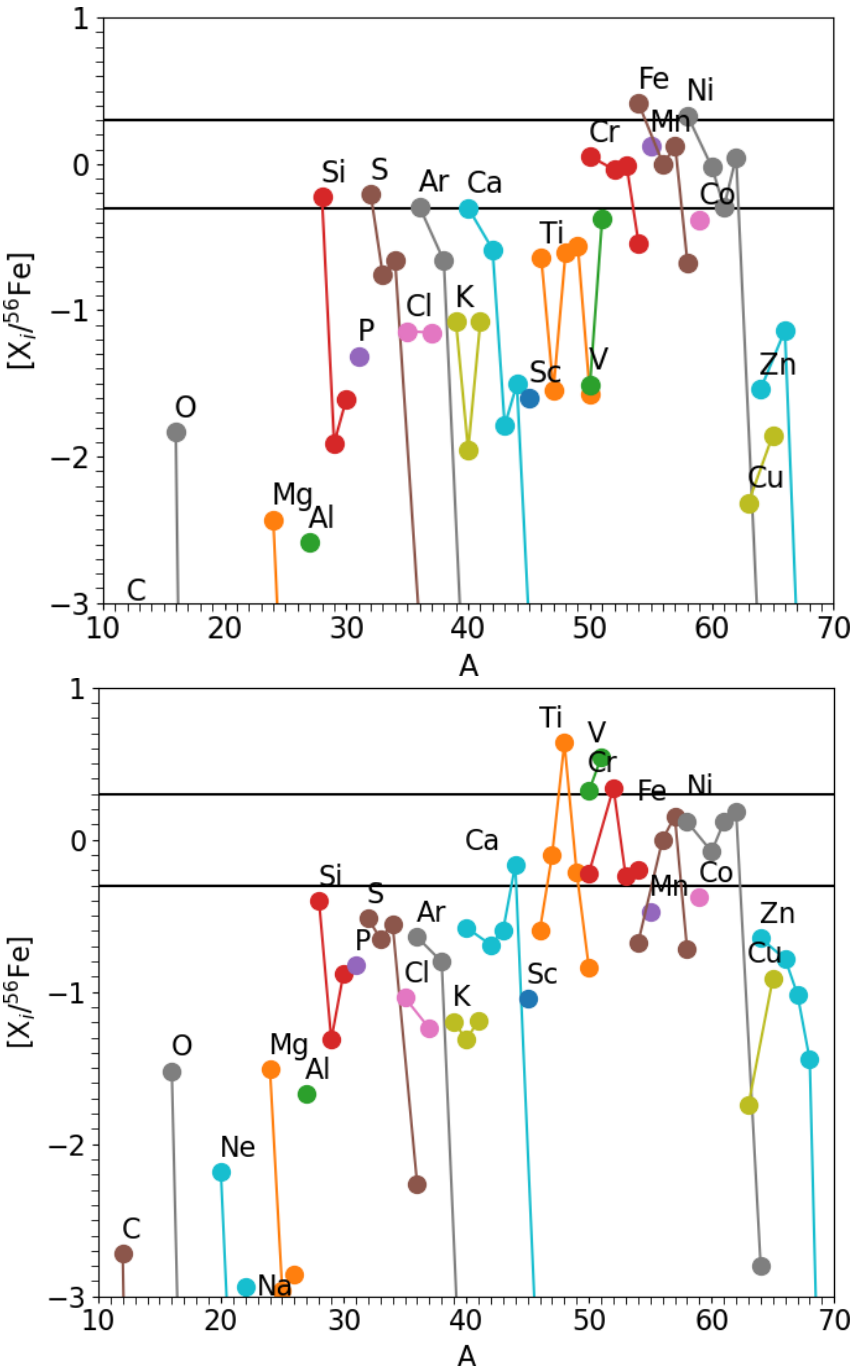

Fig. 10. (top panel) The final chemical abundance pattern of the typical Ch-mass WD[22] assuming the aspherical explosion. (bottom panel) Same as the top panel but for the typical subCh-mass WD.[35] $[X_i/^{56}\mathrm{Fe}] = \log_{10}[(X_i/^{56}\mathrm{Fe})\ /\ (X_i/^{56}\mathrm{Fe})_{\odot}]$. The two horizontal lines correspond to 50% and 200% of the solar value.

Both Ch-mass and subCh-mass WDs share some common features. They are responsible for the production of intermediate mass elements (IMEs) from Si to Ca, and the iron-peak elements from Ti to Ni. Odd number elements of IMEs are underproduced in SNe Ia. Some individual features allow us to distinguish the two models. (1) The aspherical explosion of the subCh-mass model can lead to signatures of strong Ti, V and Cr. (2) Mn is well-produced in the Ch-mass model but not in the subCh-mass model.

3. Applications of Nucleosynthesis

We have surveyed the major differences of the nucleosynthetic signature between the Ch-mass and subCh-mass WDs. Comparisons with observational data allow us to understand the progenitors of observed SNe Ia, which directly constrains the modeling. We can compare the optical signatures directly (i.e., light curves and spectra) by matching the radiative transfer model with SN Ia data.[41,60] One can also extract the chemical abundances from the spectra, and compare with nucleosynthetic results.[62,78] We shall focus on the latter method here.

3.1. *Supernova Remnant Sagittarius A East*

Within thousand years after the SN explosion, the shock-heated gas remains observable in the X-ray band, where the spectra reveal the metal composition inside the ejecta. Such a technique has been applied to the study of galactic supernova remnants (SNRs) including Tycho,[80] Kepler[81] and N103B.[82]

In Ref. 79 the SNR in Sagittarius A (Sgr A) East (G0.0+0.0) is observed based on the X-ray data taken by the *Chandra* telescope. The observed abundance ratios relative to Fe (with respect to the solar ratios) [Xi/Fe] are shown in Figure 11. The SNR features sub-solar intermediate mass elements (IMEs) and slightly super-solar iron-peak elements (Cr, Mn, and Ni).

The sub-solar IMEs exclude the possibility of associating a core-collapse SN as the origin of this remnant. On the left panel, the abundances of two distinctive classes of models, the subCh-mass and Ch-mass DDT models are plotted. The model uncertainties are shown by the shaded area. The subCh-mass models clearly overproduce the IME. Among the Ch-mass DDT models, the model that produces enough Mn and Ni overproduces Cr and the IME. There is a model whose Cr and Ni are consistent with the data points and IMEs are marginal, but its Mn is too small.

The Ch-mass PTD model (i.e., no DDT) with the initial central density of $\sim 5 \times 10^9$ g cm^{-3} is shown to be compatible with the data (right panel of Figure 11). [Such a high central density is realized in the rotating WD model.[83]] Note that this Ch-mass PTD model can well-explain the observed features of SNe Iax. Thus this object is the first identified SN Iax in the Milky Way Galaxy observed as SNR. This example also shows how the abundance guides us to identify the explosion mechanism.

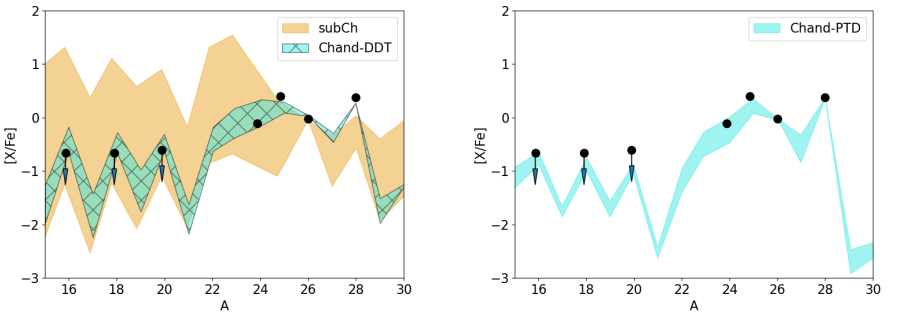

Fig. 11. (left panel) The chemical abundance pattern of the supernova remnant (SNR) Sagittarius A (from Ref. 79) for the data points compared with those of the subCh-mass[35] and Ch-mass DDT[22] models shown by the shaded regions. (right panel) Same as the left panel but for the Ch-mass PTD[15] models.

3.2. *Supernova Remnant 3C 397*

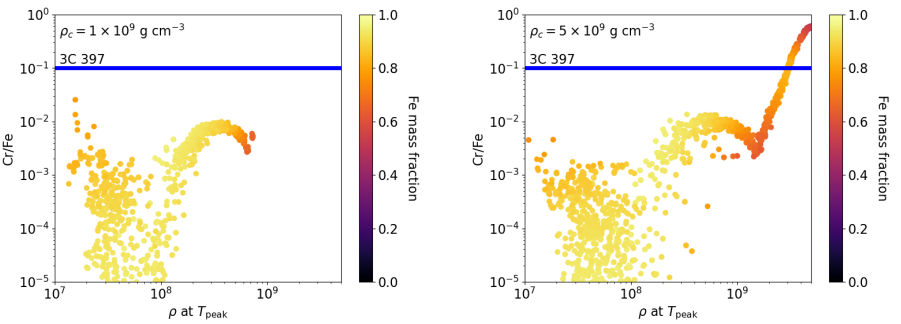

Fig. 12. (left panel) The Cr/Fe distribution of the tracers taken from the Ch-mass model with the initial central density 1×10^9 g cm^{-3}.[22] The color represents the tracer Fe mass fraction. The horizontal line is the measured value in SNR 3C 397 from Ref. 84. (right panel) Same as the left panel but for the model with the initial central density 5×10^9 g cm^{-3}.

The SNR 3C 397 is a nearby object (8 kpc) on the galactic plane. Its close distance allows astronomers to extract the spectra from individual parts similar to Sgr A. This object features a high Mn/Ni ratio, which is a key evidence of the Ch-mass explosion.[85]

In a recent observation using the *XMM-Newton* telescope, the spectra from the South and West hot blobs are measured, which give the constraint on the Cr/Fe mass ratio $\sim 0.106 \pm^{0.011}_{0.009}$.[84] The high value is used to distinguish the explosion progenitor shown in Figure 12. By comparing the tracer in different Ch-mass models, it becomes clear that the low-mass model ($\rho_c = 1 \times 10^9$ g cm^{-3}) does not have tracers reaching the observed high value. Meanwhile the high density tail in the high-mass model

($\rho_c = 5 \times 10^9$ g cm^{-3}) has tracers crossing the expected value. This provides a strong indication that this object is the explosion of the high-mass Ch-mass WD. This also demonstrates how a precise measurement of element abundance ratios can guide us to select the potential progenitor.

3.3. *Milky Way Galaxy*

In the last two sections we have shown how the SNR abundance determines its progenitor and the explosion mechanism. While there is no distinctive SNR showing chemical abundances exclusively for subCh-mass WD models, it is possible that a large sample size is needed to understand the distribution of each model. To understand the SN Ia explosion globally, we need the chemical abundances from a larger system, for example, the Milky Way Galaxy. The elements ejected by supernovae become the building block of the next-generation stars.[6] The surface abundance of stars in the solar neighbourhood may thus indicate how much each element is ejected by generations of SNe Ia.

In Ref. 86 the galactic chemical evolution model is computed with supernova abundance patterns taken from literatures. The Mn/Fe evolution is plotted in Figure 13. Two contrasting classes of models are shown, one assuming the pure Ch-mass WD explosion, and the other two assuming pure subCh-mass WD. To reproduce the trend as well as the magnitude of the data, a non-negligible fraction of the Ch-mass WD is necessary.

We remark that the supernova history can be strongly dependent on the galaxy evolution history. Some galaxies (e.g., Sculptor dwarf spheroidal galaxy) have a low Mn/Fe ratio that indicates the dominance of the subCh-mass WD explosion in their evolution histories.[90,91] Meanwhile, some early rise of [Mn/Fe] in this subclass of galaxies can be a result of the Ch-mass SN Iax explosion.[92]

3.4. *Perseus Galactic Cluster*

The Milky Way Galaxy can provide a detailed reference in how generations of stars contributes to the cosmic metal enrichment. However, large N-body simulations suggest that each galaxy is unique in their evolution history. To understand how each supernova model contributes in the cosmic scale, data from an even larger system is important to average out the statistical fluctuations of individual galaxies.

In Ref. 93 the X-ray spectra of the Perseus Cluster is studied by the *Hitomi* telescope. The highly resolved spectral lines provide the abundance measurement with uncertainties down to $\sim 10\%$. The high precision can distinguish supernova models and mechanisms explicitly. The fitting using SN Ia and CCSN models from literature is shown in Table 3. The best-fit model is found to be the scenario assuming pure Ch-mass WD explosion. If the fraction of the Ch-mass WD is relaxed as a model parameter, the expected Ch-mass WD still contributes about $10 - 40\%$ of the SN Ia population, depending on the exact CCSN models.

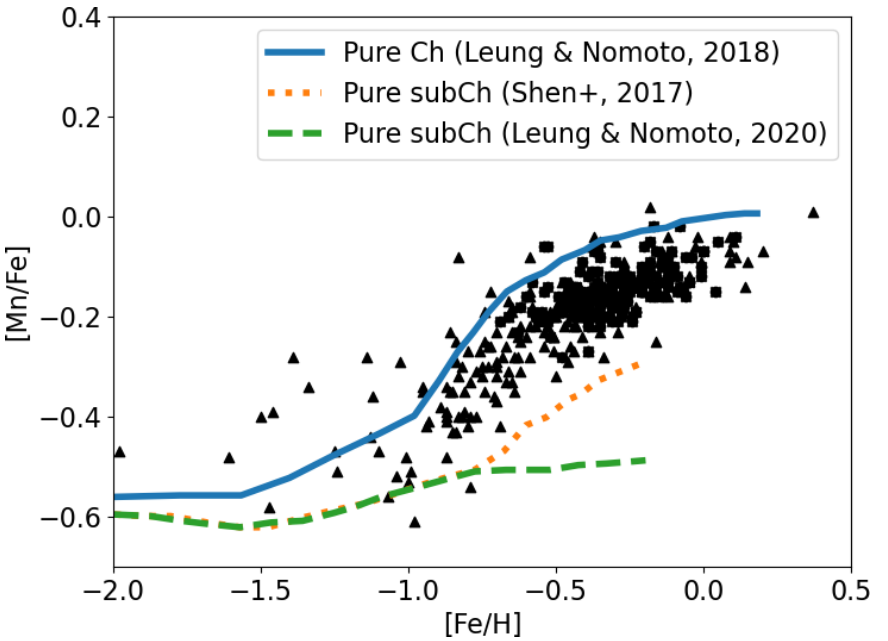

Fig. 13. The [Mn/Fe] against metallicity [Fe/H] for the galactic chemical evolution models taken from Ref. 86. Solid lines come from theoretical models assuming pure Ch-mass and subCh-mass explosion history. Data points are the stellar abundances from the solar neighbourhood.[87–89]

Table 3. Models assuming different stellar and supernova models and their corresponding (Ch-mass) SN Ia rates (data taken from [Ref. 93]).

Model	$f_{\rm Ia}$	$f_{\rm Chand}$	χ^2
pure Ch-mass[Ref. 22]+ CCSN[Ref. 94]	0.21 ± 0.02	N/A	11.78
Ch-mass[Ref. 95] + subCh-mass[Ref. 32] + CCSN[94]	0.25 ± 0.06	0.36 ± 0.14	23.96
Ch-mass[Ref. 95] + subCh-mass[Ref. 32] + CCSN[96]	0.38 ± 0.06	0.09 ± 0.09	15.73

4. Conclusion

In this review article we have presented the physical background about the Ch-mass and subCh-mass WD models as the SN Ia explosion progenitors. We discussed the differences in their explosion mechanisms and their associated nucleosynthetic signatures. We have also demonstrated how the chemical abundances of SNRs, Milky Way Galaxy, and galactic clusters can help us distinguish (1) the individual SN explosion scenario and (2) the relative importance of each explosion model.

Nucleosynthesis will remain an important subject in the future supernova study thanks to observational projects such as XRISM (X-Ray Imaging and Spectroscopy Mission). Given the power of resolving spectral lines as its predecessor *Hitomi*, we can anticipate that the high quality spectral data, and hence the precise chemical

abundance measurements, will shed light on supernova models to an unprecedented accuracy.

Acknowledgments

S.C.L. thanks the session chairpersons Pilar-Ruiz Lapuente and Robert Fisher for the invition to the introductory talk in the Marcel Grossmann 16 Meeting. S.C.L acknowledges support by NASA grants HST-AR-15021.001-A and 80NSSC18K1017. K.N. has been supported by the World Premier International Research Center Initiative (WPI Initiative), MEXT, Japan, and JSPS KAKENHI Grant Numbers JP17K05382, JP20K04024, and JP21H04499.

References

1. W. D. Arnett, A Possible Model of Supernovae: Detonation of ^{12}C, *Astrophysics and Space Science* **5**, 180 (October 1969).
2. W. Hillebrandt and J. C. Niemeyer, Type IA Supernova Explosion Models, *Annual Review of Astronomy and Astrophysics* **38**, 191 (January 2000).
3. K. Nomoto and S.-C. Leung, *Thermonuclear Explosions of Chandrasekhar Mass White Dwarfs*, in *Handbook of Supernovae*, eds. A. W. Alsabti and P. Murdin 2017, p. 1275.
4. A. G. Riess, A. V. Filippenko, P. Challis, A. Clocchiatti, A. Diercks, P. M. Garnavich, R. L. Gilliland, C. J. Hogan, S. Jha, R. P. Kirshner, B. Leibundgut, M. M. Phillips, D. Reiss, B. P. Schmidt, R. A. Schommer, R. C. Smith, J. Spyromilio, C. Stubbs, N. B. Suntzeff and J. Tonry, Observational Evidence from Supernovae for an Accelerating Universe and a Cosmological Constant, *Astronomical Journal* **116**, 1009 (September 1998).
5. S. Perlmutter, G. Aldering, G. Goldhaber, R. A. Knop, P. Nugent, P. G. Castro, S. Deustua, S. Fabbro, A. Goobar, D. E. Groom, I. M. Hook, A. G. Kim, M. Y. Kim, J. C. Lee, N. J. Nunes, R. Pain, C. R. Pennypacker, R. Quimby, C. Lidman, R. S. Ellis, M. Irwin, R. G. McMahon, P. Ruiz-Lapuente, N. Walton, B. Schaefer, B. J. Boyle, A. V. Filippenko, T. Matheson, A. S. Fruchter, N. Panagia, H. J. M. Newberg, W. J. Couch and T. S. C. Project, Measurements of Ω and Λ from 42 High-Redshift Supernovae, *Astrophysical Journal* **517**, 565 (June 1999).
6. F. Matteucci, *The chemical evolution of the Galaxy* 2001.
7. C. Kobayashi, A. I. Karakas and H. Umeda, The evolution of isotope ratios in the Milky Way Galaxy, *Monthly Notices of the Royal Astronomical Society* **414**, 3231 (July 2011).
8. K. Nomoto, D. Sugimoto and S. Neo, Carbon Deflagration Supernova, an Alternative to Carbon Detonation, *Astrophysics and Space Science* **39**, p. L37 (February 1976).
9. K. Nomoto, F. K. Thielemann and K. Yokoi, Accreting white dwarf models for type I supern. III. Carbon deflagration supernovae., *Astrophysical Journal* **286**, 644 (November 1984).
10. E. Livne, Numerical Simulations of the Convective Flame in White Dwarfs, *Astrophysical Journal Letter* **406**, p. L17 (March 1993).
11. M. Reinecke, W. Hillebrandt and J. C. Niemeyer, Thermonuclear explosions of Chandrasekhar-mass C+O white dwarfs, *Astronomy and Astrophysics* **347**, 739 (July 1999).

12. M. Reinecke, W. Hillebrandt and J. C. Niemeyer, Refined numerical models for multidimensional type Ia supernova simulations, *Astronomy and Astrophysics* **386**, 936 (May 2002).
13. F. K. Röpke, W. Hillebrandt, W. Schmidt, J. C. Niemeyer, S. I. Blinnikov and P. A. Mazzali, A Three-Dimensional Deflagration Model for Type Ia Supernovae Compared with Observations, *Astrophysical Journal* **668**, 1132 (October 2007).
14. H. Ma, S. E. Woosley, C. M. Malone, A. Almgren and J. Bell, Carbon Deflagration in Type Ia Supernova. I. Centrally Ignited Models, *Astrophysical Journal* **771**, p. 58 (July 2013).
15. S.-C. Leung and K. Nomoto, Explosive Nucleosynthesis in Near-Chandrasekhar Mass White Dwarf Models for Type Iax Supernovae: Dependence on Model Parameters, *Astrophysical Journal* **900**, p. 54 (September 2020).
16. A. M. Khokhlov, Delayed detonation model for type IA supernovae, *Astronomy and Astrophysics* **245**, 114 (May 1991).
17. H. Yamaoka, K. Nomoto, T. Shigeyama and F.-K. Thielemann, Late Detonation Models for the Type IA Supernovae SN 1991T and SN 1990N, *Astrophysical Journal Letter* **393**, p. L55 (July 1992).
18. K. Iwamoto, F. Brachwitz, K. Nomoto, N. Kishimoto, H. Umeda, W. R. Hix and F.-K. Thielemann, Nucleosynthesis in Chandrasekhar Mass Models for Type IA Supernovae and Constraints on Progenitor Systems and Burning-Front Propagation, *Astrophysical Journal Supplementary* **125**, 439 (December 1999).
19. I. Golombek and J. C. Niemeyer, A model for multidimensional delayed detonations in SN Ia explosions, *Astronomy and Astrophysics* **438**, 611 (August 2005).
20. F. K. Röpke and J. C. Niemeyer, Delayed detonations in full-star models of type Ia supernova explosions, *Astronomy and Astrophysics* **464**, 683 (March 2007).
21. M. Fink, M. Kromer, I. R. Seitenzahl, F. Ciaraldi-Schoolmann, F. K. Röpke, S. A. Sim, R. Pakmor, A. J. Ruiter and W. Hillebrandt, Three-dimensional pure deflagration models with nucleosynthesis and synthetic observables for Type Ia supernovae, *Monthly Notices of the Royal Astronomical Society* **438**, 1762 (February 2014).
22. S.-C. Leung and K. Nomoto, Explosive Nucleosynthesis in Near-Chandrasekhar-mass White Dwarf Models for Type Ia Supernovae: Dependence on Model Parameters, *Astrophysical Journal* **861**, p. 143 (July 2018).
23. T. Plewa, A. C. Calder and D. Q. Lamb, Type Ia Supernova Explosion: Gravitationally Confined Detonation, *Astrophysical Journal Letter* **612**, L37 (September 2004).
24. C. A. Meakin, I. Seitenzahl, D. Townsley, I. Jordan, George C., J. Truran and D. Lamb, Study of the Detonation Phase in the Gravitationally Confined Detonation Model of Type Ia Supernovae, *Astrophysical Journal* **693**, 1188 (March 2009).
25. I. Jordan, G. C., C. Graziani, R. T. Fisher, D. M. Townsley, C. Meakin, K. Weide, L. B. Reid, J. Norris, R. Hudson and D. Q. Lamb, The Detonation Mechanism of the Pulsationally Assisted Gravitationally Confined Detonation Model of Type Ia Supernovae, *Astrophysical Journal* **759**, p. 53 (November 2012).
26. D. García-Senz, R. M. Cabezón, I. Domínguez and F. K. Thielemann, Type Ia Supernovae: Can Coriolis Force Break the Symmetry of the Gravitational Confined Detonation Explosion Mechanism?, *Astrophysical Journal* **819**, p. 132 (March 2016).
27. I. R. Seitenzahl, M. Kromer, S. T. Ohlmann, F. Ciaraldi-Schoolmann, K. Marquardt, M. Fink, W. Hillebrandt, R. Pakmor, F. K. Röpke, A. J. Ruiter, S. A. Sim and S. Taubenberger, Three-dimensional simulations of gravitationally confined detonations compared to observations of SN 1991T, *Astronomy and Astrophysics* **592**, p. A57 (July 2016).

28. E. Bravo, D. García-Senz, R. M. Cabezon and I. Domnguez, Pulsating Reverse Detonation Models of Type Ia Supernovae. I. Detonation Ignition, Astrophysical Journal 695, 1244 (April 2009).
29. E. Bravo, D. García-Senz, R. M. Cabezón and I. Domínguez, Pulsating Reverse Detonation Models of Type Ia Supernovae. II. Explosion, *Astrophysical Journal* **695**, 1257 (April 2009).
30. K. Nomoto, Accreting white dwarf models for type I supernovae. II. Off-center detonation supernovae, *Astrophysical Journal* **257**, 780 (June 1982).
31. M. Fink, F. K. Röpke, W. Hillebrandt, I. R. Seitenzahl, S. A. Sim and M. Kromer, Double-detonation sub-Chandrasekhar supernovae: Can minimum helium shell masses detonate the core?, *Astronomy and Astrophysics* **514**, p. A53 (May 2010).
32. K. J. Shen, D. Kasen, B. J. Miles and D. M. Townsley, Sub-Chandrasekhar-mass White Dwarf Detonations Revisited, *Astrophysical Journal* **854**, p. 52 (February 2018).
33. A. Tanikawa, K. Nomoto and N. Nakasato, Three-dimensional Simulation of Double Detonations in the Double-degenerate Model for Type Ia Supernovae and Interaction of Ejecta with a Surviving White Dwarf Companion, *Astrophysical Journal* **868**, p. 90 (December 2018).
34. A. Tanikawa, K. Nomoto, N. Nakasato and K. Maeda, Double-detonation Models for Type Ia Supernovae: Trigger of Detonation in Companion White Dwarfs and Signatures of Companions' Stripped-off Materials, *Astrophysical Journal* **885**, p. 103 (November 2019).
35. S.-C. Leung and K. Nomoto, Explosive Nucleosynthesis in Sub-Chandrasekhar-mass White Dwarf Models for Type Ia Supernovae: Dependence on Model Parameters, *Astrophysical Journal* **888**, p. 80 (January 2020).
36. A. Polin, P. Nugent and D. Kasen, Nebular Models of Sub-Chandrasekhar Mass Type Ia Supernovae: Clues to the Origin of Ca-rich Transients, *Astrophysical Journal* **906**, p. 65 (January 2021).
37. K. J. Shen, S. Blondin, D. Kasen, L. Dessart, D. M. Townsley, S. Boos and D. J. Hillier, Non-local Thermodynamic Equilibrium Radiative Transfer Simulations of Sub-Chandrasekhar-mass White Dwarf Detonations, *Astrophysical Journal Letter* **909**, p. L18 (March 2021).
38. S. Gronow, C. E. Collins, S. A. Sim and F. K. Röpke, Double detonations of sub-M_{Ch} CO white dwarfs: Variations in Type Ia supernovae due to different core and He shell masses, *Astronomy and Astrophysics* **649**, p. A155 (May 2021).
39. R. Pakmor, S. Hachinger, F. K. Röpke and W. Hillebrandt, Violent mergers of nearly equal-mass white dwarf as progenitors of subluminous Type Ia supernovae, *Astronomy and Astrophysics* **528**, p. A117 (April 2011).
40. R. Pakmor, M. Kromer, S. Taubenberger, S. A. Sim, F. K. Röpke and W. Hillebrandt, Normal Type Ia Supernovae from Violent Mergers of White Dwarf Binaries, *Astrophysical Journal Letter* **747**, p. L10 (March 2012).
41. M. Kromer, R. Pakmor, S. Taubenberger, G. Pignata, M. Fink, F. K. Röpke, I. R. Seitenzahl, S. A. Sim and W. Hillebrandt, SN 2010lp—A Type Ia Supernova from a Violent Merger of Two Carbon-Oxygen White Dwarfs, *Astrophysical Journal Letter* **778**, p. L18 (November 2013).
42. A. Tanikawa, N. Nakasato, Y. Sato, K. Nomoto, K. Maeda and I. Hachisu, Hydrodynamical Evolution of Merging Carbon-Oxygen White Dwarfs: Their Pre-supernova Structure and Observational Counterparts, *Astrophysical Journal* **807**, p. 40 (July 2015).
43. D. García-Senz, R. M. Cabezón, A. Arcones, A. Relaño and F. K. Thielemann, High-resolution simulations of the head-on collision of white dwarfs, *Monthly Notices of the Royal Astronomical Society* **436**, 3413 (December 2013).

44. D. Kushnir, B. Katz, S. Dong, E. Livne and R. Fernández, Head-on Collisions of White Dwarfs in Triple Systems Could Explain Type Ia Supernovae, *Astrophysical Journal Letter* **778**, p. L37 (December 2013).
45. O. Papish and H. B. Perets, Supernovae from Direct Collisions of White Dwarfs and the Role of Helium Shell Ignition, *Astrophysical Journal* **822**, p. 19 (May 2016).
46. U. Das and B. Mukhopadhyay, Maximum mass of stable magnetized highly super-Chandrasekhar white dwarfs: Stable solutions with varying magnetic fields, *Journal of Cosmology and Astroparticle Physics* **2014**, p. 050 (June 2014).
47. Y. Kamiya, M. Tanaka, K. Nomoto, S. I. Blinnikov, E. I. Sorokina and T. Suzuki, Super-Chandrasekhar-mass Light Curve Models for the Highly Luminous Type Ia Supernova 2009dc, *Astrophysical Journal* **756**, p. 191 (September 2012).
48. S. C. Yoon and N. Langer, On the evolution of rapidly rotating massive white dwarfs towards supernovae or collapses, *Astronomy and Astrophysics* **435**, 967 (June 2005).
49. I. Hachisu, M. Kato, H. Saio and K. Nomoto, A Single Degenerate Progenitor Model for Type Ia Supernovae Highly Exceeding the Chandrasekhar Mass Limit, *Astrophysical Journal* **744**, p. 69 (January 2012).
50. S. C. Leung, M. C. Chu and L. M. Lin, Dark Matter Admixed Type Ia Supernovae, *Astrophysical Journal* **812**, p. 110 (October 2015).
51. H.-S. Chan, M.-c. Chu, S.-C. Leung and L.-M. Lin, Delayed Detonation Thermonuclear Supernovae with an Extended Dark Matter Component, *Astrophysical Journal* **914**, p. 138 (June 2021).
52. K. Nomoto and S.-C. Leung, Single Degenerate Models for Type Ia Supernovae: Progenitor's Evolution and Nucleosynthesis Yields, *Space Science Review* **214**, p. 67 (June 2018).
53. K. Nomoto, Accreting white dwarf models for type I supernovae. I - Presupernova evolution and triggering mechanisms, *Astrophysical Journal* **253**, 798 (February 1982).
54. J. C. Niemeyer and W. Hillebrandt, Turbulent Nuclear Flames in Type IA Supernovae, *Astrophysical Journal* **452**, p. 769 (October 1995).
55. J. B. Bell, M. S. Day, C. A. Rendleman, S. E. Woosley and M. Zingale, Direct Numerical Simulations of Type Ia Supernovae Flames. I. The Landau-Darrieus Instability, *Astrophysical Journal* **606**, 1029 (May 2004).
56. J. B. Bell, M. S. Day, C. A. Rendleman, S. E. Woosley and M. Zingale, Direct Numerical Simulations of Type Ia Supernovae Flames. II. The Rayleigh-Taylor Instability, *Astrophysical Journal* **608**, 883 (June 2004).
57. R. Fisher and K. Jumper, Single-degenerate Type Ia Supernovae Are Preferentially Overluminous, *Astrophysical Journal* **805**, p. 150 (June 2015).
58. J. C. Niemeyer and W. Hillebrandt, Microscopic Instabilities of Nuclear Flames in Type IA Supernovae, *Astrophysical Journal* **452**, p. 779 (October 1995).
59. S. E. Woosley, Neutron-rich Nucleosynthesis in Carbon Deflagration Supernovae, *Astrophysical Journal* **476**, 801 (February 1997).
60. O. Graur, D. Zurek, M. M. Shara, A. G. Riess, I. R. Seitenzahl and A. Rest, Late-time Photometry of Type Ia Supernova SN 2012cg Reveals the Radioactive Decay of 57 Co, *Astrophysical Journal* **819**, p. 31 (March 2016).
61. B. J. Shappee, K. Z. Stanek, C. S. Kochanek and P. M. Garnavich, Whimper of a Bang: Documenting the Final Days of the Nearby Type Ia Supernova 2011fe, *Astrophysical Journal* **841**, p. 48 (May 2017).
62. K. Mori, M. A. Famiano, T. Kajino, T. Suzuki, P. M. Garnavich, G. J. Mathews, R. Diehl, S.-C. Leung and K. Nomoto, Nucleosynthesis Constraints on the Explosion Mechanism for Type Ia Supernovae, *Astrophysical Journal* **863**, p. 176 (August 2018).
63. D. Kasen, F. K. Röpke and S. E. Woosley, The diversity of type Ia supernovae from broken symmetries, *Nature* **460**, 869 (August 2009).

64. I. R. Seitenzahl, G. Cescutti, F. K. Röpke, A. J. Ruiter and R. Pakmor, Solar abundance of manganese: A case for near Chandrasekhar-mass Type Ia supernova progenitors, *Astronomy and Astrophysics* **559**, p. L5 (November 2013).
65. A. M. Lisewski, W. Hillebrandt and S. E. Woosley, Constraints on the Delayed Transition to Detonation in Type IA Supernovae, *Astrophysical Journal* **538**, 831 (August 2000).
66. F. K. Röpke, Flame-driven Deflagration-to-Detonation Transitions in Type Ia Supernovae?, *Astrophysical Journal* **668**, 1103 (October 2007).
67. S. E. Woosley, A. R. Kerstein, V. Sankaran, A. J. Aspden and F. K. Röpke, Type Ia Supernovae: Calculations of Turbulent Flames Using the Linear Eddy Model, *Astrophysical Journal* **704**, 255 (October 2009).
68. D. Fenn, T. Plewa and A. Gawryszczak, No double detonations but core carbon ignitions in high-resolution, grid-based simulations of binary white dwarf mergers, *Monthly Notices of the Royal Astronomical Society* **462**, 2486 (November 2016).
69. E. Brooker, T. Plewa and D. Fenn, Type Ia supernovae deflagration-to-detonation transition explosions powered by the Zel'dovich reactivity gradient mechanism, *Monthly Notices of the Royal Astronomical Society* **501**, L23 (January 2021).
70. S. C. Leung, M. C. Chu and L. M. Lin, A new hydrodynamics code for Type Ia supernovae, *Monthly Notices of the Royal Astronomical Society* **454**, 1238 (December 2015).
71. S. Nagataki, T. M. Shimizu and K. Sato, Matter Mixing from Axisymmetric Supernova Explosion, *Astrophysical Journal* **495**, 413 (March 1998).
72. C. Travaglio, W. Hillebrandt, M. Reinecke and F. K. Thielemann, Nucleosynthesis in multi-dimensional SN Ia explosions, *Astronomy and Astrophysics* **425**, 1029 (October 2004).
73. I. R. Seitenzahl, F. K. Röpke, M. Fink and R. Pakmor, Nucleosynthesis in thermonuclear supernovae with tracers: Convergence and variable mass particles, *Monthly Notices of the Royal Astronomical Society* **407**, 2297 (October 2010).
74. D. M. Townsley, B. J. Miles, F. X. Timmes, A. C. Calder and E. F. Brown, A Tracer Method for Computing Type Ia Supernova Yields: Burning Model Calibration, Reconstruction of Thickened Flames, and Verification for Planar Detonations, *Astrophysical Journal Supplementary* **225**, p. 3 (July 2016).
75. F. X. Timmes, Integration of Nuclear Reaction Networks for Stellar Hydrodynamics, *Astrophysical Journal Supplementary* **124**, 241 (September 1999).
76. F. K. Thielemann, K. Nomoto, and K. Yokoi, Explosive nucleosynthesis in carbon deflagration models of Type I supernovae, *Astronomy and Astrophysics* **158**, 17 (April 1986).
77. F. Lach, F. K. Röpke, I. R. Seitenzahl, B. Coté, S. Gronow and A. J. Ruiter, Nucleosynthesis imprints from different Type Ia supernova explosion scenarios and implications for galactic chemical evolution, *Astronomy and Astrophysics* **644**, p. A118 (December 2020).
78. S.-C. Leung, R. Diehl, K. Nomoto and T. Siegert, Exploration of Aspherical Ejecta Properties in Type Ia Supernovae: Progenitor Dependence and Applications to Progenitor Classification, *Astrophysical Journal* **909**, p. 152 (March 2021).
79. P. Zhou, S.-C. Leung, Z. Li, K. Nomoto, J. Vink and Y. Chen, Chemical Abundances in Sgr A East: Evidence for a Type Iax Supernova Remnant, *Astrophysical Journal* **908**, p. 31 (February 2021).
80. S. Park, C. Badenes, K. Mori, R. Kaida, E. Bravo, A. Schenck, K. A. Eriksen, J. P. Hughes, P. O. Slane, D. N. Burrows and J.-J. Lee, A Super-solar Metallicity for the Progenitor of Kepler's Supernova, *Astrophysical Journal Letter* **767**, p. L10 (April 2013).

81. H. Yamaguchi, J. P. Hughes, C. Badenes, E. Bravo, I. R. Seitenzahl, H. Martínez-Rodríguez, S. Park and R. Petre, The Origin of the Iron-rich Knot in Tycho's Supernova Remnant, *Astrophysical Journal* **834**, p. 124 (January 2017).
82. H. Yamaguchi, F. Acero, C.-J. Li and Y.-H. Chu, Discovery of Double-ring Structure in the Supernova Remnant N103B: Evidence for Bipolar Winds from a Type Ia Supernova Progenitor, *Astrophysical Journal Letter* **910**, p. L24 (April 2021).
83. O. G. Benvenuto, J. A. Panei, K. Nomoto, H. Kitamura and I. Hachisu, Final Evolution and Delayed Explosions of Spinning White Dwarfs in Single Degenerate Models for Type Ia Supernovae, *Astrophysical Journal Letter* **809**, p. L6 (August 2015).
84. Y. Ohshiro, H. Yamaguchi, S.-C. Leung, K. Nomoto, T. Sato, T. Tanaka, H. Okon, R. Fisher, R. Petre and B. J. Williams, Discovery of a Highly Neutronized Ejecta Clump in the Type Ia Supernova Remnant 3C 397, *Astrophysical Journal Letter* **913**, p. L34 (June 2021).
85. H. Yamaguchi, C. Badenes, A. R. Foster, E. Bravo, B. J. Williams, K. Maeda, M. Nobukawa, K. A. Eriksen, N. S. Brickhouse, R. Petre and K. Koyama, A Chandrasekhar Mass Progenitor for the Type Ia Supernova Remnant 3C 397 from the Enhanced Abundances of Nickel and Manganese, *Astrophysical Journal Letter* **801**, p. L31 (March 2015).
86. C. Kobayashi, S.-C. Leung and K. Nomoto, New Type Ia Supernova Yields and the Manganese and Nickel Problems in the Milky Way and Dwarf Spheroidal Galaxies, *Astrophysical Journal* **895**, p. 138 (June 2020).
87. B. E. Reddy, J. Tomkin, D. L. Lambert and C. Allende Prieto, The chemical compositions of Galactic disc F and G dwarfs, *Monthly Notices of the Royal Astronomical Society* **340**, 304 (March 2003).
88. B. E. Reddy, D. L. Lambert and C. Allende Prieto, Elemental abundance survey of the Galactic thick disc, *Monthly Notices of the Royal Astronomical Society* **367**, 1329 (April 2006).
89. S. Feltzing, M. Fohlman and T. Bensby, Manganese trends in a sample of thin and thick disk stars. The origin of Mn, *Astronomy and Astrophysics* **467**, 665 (May 2007).
90. E. N. Kirby, J. L. Xie, R. Guo, M. A. C. de los Reyes, M. Bergemann, M. Kovalev, K. J. Shen, A. L. Piro and A. McWilliam, Evidence for Sub-Chandrasekhar Type Ia Supernovae from Stellar Abundances in Dwarf Galaxies, *Astrophysical Journal* **881**, p. 45 (August 2019).
91. M. A. C. de los Reyes, E. N. Kirby, I. R. Seitenzahl and K. J. Shen, Manganese Indicates a Transition from Sub- to Near-Chandrasekhar Type Ia Supernovae in Dwarf Galaxies, *Astrophysical Journal* **891**, p. 85 (March 2020).
92. C. Kobayashi, K. Nomoto and I. Hachisu, Subclasses of Type Ia Supernovae as the Origin of [α/Fe] Ratios in Dwarf Spheroidal Galaxies, *Astrophysical Journal Letter* **804**, p. L24 (May 2015).
93. A. Simionescu, S. Nakashima, H. Yamaguchi, K. Matsushita, F. Mernier, N. Werner, T. Tamura, K. Nomoto, J. de Plaa, S. C. Leung, A. Bamba, E. Bulbul, M. E. Eckart, Y. Ezoe, A. C. Fabian, Y. Fukazawa, L. Gu, Y. Ichinohe, M. N. Ishigaki, J. S. Kaastra, C. Kilbourne, T. Kitayama, M. Leutenegger, M. Loewenstein, Y. Maeda, E. D. Miller, R. F. Mushotzky, H. Noda, C. Pinto, F. S. Porter, S. Safi-Harb, K. Sato, T. Takahashi, S. Ueda and S. Zha, Constraints on the chemical enrichment history of the Perseus Cluster of galaxies from high-resolution X-ray spectroscopy, *Monthly Notices of the Royal Astronomical Society* **483**, 1701 (February 2019).

94. K. Nomoto, C. Kobayashi and N. Tominaga, Nucleosynthesis in Stars and the Chemical Enrichment of Galaxies, *Annual Review of Astronomy and Astrophysics* **51**, 457 (August 2013).
95. I. R. Seitenzahl, F. Ciaraldi-Schoolmann, F. K. Röpke, M. Fink, W. Hillebrandt, M. Kromer, R. Pakmor, A. J. Ruiter, S. A. Sim and S. Taubenberger, Three-dimensional delayed-detonation models with nucleosynthesis for Type Ia supernovae, *Monthly Notices of the Royal Astronomical Society* **429**, 1156 (February 2013).
96. T. Sukhbold, T. Ertl, S. E. Woosley, J. M. Brown and H. T. Janka, Core-collapse Supernovae from 9 to 120 Solar Masses Based on Neutrino-powered Explosions, *Astrophysical Journal* **821**, p. 38 (April 2016).